Chapter

Study of Bio-Based Foams Prepared from PBAT/PLA Reinforced with Bio-Calcium Carbonate and Compatibilized with Gamma Radiation

Elizabeth C.L. Cardoso, Duclerc F. Parra, Sandra R. Scagliusi, Ricardo M. Sales, Fernando Caviquioli and Ademar B. Lugão

Abstract

Foamed polymers are future materials, considered "green materials" due to their properties with very low consumption of raw materials; they can be used to ameliorate appearance of structures besides contributing for thermal and acoustic insulation. Nevertheless, waste disposal has generated about 20–30% of total of solid volume in landfills besides prejudicing flora and fauna by uncontrolled disposal. The development of biodegradable polymers aims to solve this problem, considering that in 2012, bio-plastics market was evaluated in 1.4 million tons produced and in 2017 attained 6.2 million tons. Biodegradable polymers as poly(lactic acid) (PLA) and poly(butylene adipate-*co*-terephthalate) (PBAT) are thermoplastics which can be processed using the most conventional polymer processing methods. PLA is high in strength and modulus but brittle, while PBAT is flexible and tough. In order to reduce interfacial tension exhibited by PLA/PBAT blends, it was used as compatibilizing agent 5 phr of PLA previously gamma-radiated at 150 kGy. Ionizing radiation induces compatibilization by free radicals, improving the dispersion and adhesion of blend phases, without using chemical additives and at room temperature. As a reinforcement agent, calcium carbonate from avian eggshell waste was used, at 10 ph of micro particles, 125 μm. Admixtures were further processed in a single-screw extruder, using CO_2 as physical blowing agent (PBA). Property investigations were performed by DSC, TGA, XRD, SEM, FTIR, and mechanical essays.

Keywords: PBAT/PLA foams, eggshells, PBA, gamma radiation, compatibilization

1. Introduction

Natural polymers, biopolymers, and synthetic polymers based on annually renewable resources are the basis for the twenty-first-century portfolio of sustainable, eco-efficient plastics. The interest on these polymers is considerable, due to a decrease of world resources in oil; in addition, there is a concern to limit the plastics' contribution to waste disposal. The degree of concern has been [1–8] raised

along with the development in urbanization. The development of biodegradable polymers generally catches the attention of researchers due to environmental problems associated with the disposal of petroleum-based polymers.

The depletion of petroleum resource led to considerable research efforts on the development of biodegradable polymeric materials. Biodegradable polymers offer a great variety of advantages to environmental conservation; based on their non-harmful effects, they can be classified into two major categories: natural polymers and synthetic polymers; polymers obtained basically from renewable sources are a new generation of material capable to significantly reduce the environmental impact in order to achieve certain technical requirements besides being fully biodegradable. In addition, natural polymer-based materials offer a feasible alternative to the traditional polymeric materials when recycling of synthetic polymer is not cost-effective or technically impossible [9–15].

Poly(butylene adipate-*co*-terephthalate) (PBAT) is an aliphatic-aromatic random co-polyester, fully biodegradable, and prepared from 1,4–butanediol, adipic acid, and terephthalic acid: a synthetic polymer based on fossil resources, 100% biodegradable, with high elongation at break, and very flexible [16]. PBAT is an elastomeric polymer intended to improve mechanical properties; it can be used in several applications, such as, packaging materials, hygiene products, biomedical fields, and industrial composting, among others [17–21]; nevertheless, PBAT has poor thermal and mechanical properties, which can be overcome through the addition of fillers; in addition, it is a versatile polymer that allows the manufacturing from films up to shaped devices, and it can be used in food and dairy industries as well in hygiene packing [22, 23].

Polylactide or poly(lactic acid) (PLA) is the front-runner in the emerging bioplastics market with the best availability and the most attractive cost structure: PLA is a linear, aliphatic thermoplastic polyester, used for different applications ranging from medical to packaging, resorbable, and biodegradable under industrial composting conditions [24]. Therefore, its rheological properties, especially its shear viscosity, have important effects on thermal processes. Despite all its advantages, some properties of PLA such as inherent brittleness, low toughness, slow crystallization, poor melt strength, narrow processing window, and low thermal stability, besides high cost, pose considerable scientific challenges that limit their large-scale applications (film blowing, injection molding, and foaming) [25–27].

So, combining the high toughness of PBAT and the relatively low price of PLA can result in a novel blend. PLA was blended with PBAT flexible polymer, considering its high toughness and biodegradability. Poly(lactic acid) (PLA) and poly(butylene adipate-*co*-terephthalate) (PBAT), both biodegradable aliphatic polyesters, semicrystalline, and thermoplastic, can be processed by conventional methods. Their resulting blends provide interesting materials for industrial and hygiene packaging applications, due to their increased ductility in function of PBAT content.

PLA and PBAT binary blends exhibited improved properties concerned with higher elongation at break but lower tensile strength and modulus than pure PLA. Therefore, the addition of filler to PLA/PBAT blends led to a modulus approaching that of pure PLA.

In this paper bio-calcium carbonate from avian egg shells was used. Daily, tons of chicken eggshells are discarded, generating commercially devalued waste from restaurants, food industry, and homes. Currently, egg production throughout the world is 65.5 million metric tons per year, with Asia as a key contributor to global egg output growth [28]. The eggshell is rich in calcium carbonate, a natural bioceramic composite with a unique chemical composition of high inorganic (95% of calcium carbonate in the form of calcite) and 5% of organic (type X collagen,

sulfated polysaccharides) components; this eggshell characteristic structure combined with substantial availability makes eggshells a potential source of bio-fillers that can be efficiently used for polymer composites [29].

Unfortunately, PLA/PBAT blends filled with calcium carbonate ($CaCO_3$) have poor mechanical properties due to the poor interfacial adhesion. Many polymers are immiscible and form heterogeneous systems when blended. In order to cope with this problem, irradiation was used to improve the compatibility between immiscible polymers in a blend. In comparison with other methods of compatibilization based on the reactivity of functional groups grafted on the polymer backbone, the changes are not limited to the interface. Irradiation leads to changes not only in the interphase but also in the bulk of both polymers (chain scission, crosslinking, etc.). Therefore, it is very difficult to determine whether macroscopic properties change due to the compatibilizing effect of irradiation or due to modification of the polymers in bulk. A great number of authors working on irradiated immiscible polymer blends claim in their articles to have increased the compatibility between the two polymers just considering mechanical properties. Compatibilization is essential in order to decrease interfacial tension exhibited by PLA/PBAT blends: herein it was used as compatibilizing agent of PLA previously gamma-radiated at 150 kGy, air environment, 10.5 kGy h^{-1}. Güven and collaborators have proposed the use of ionizing radiation in replacing chemical compatibilizing agents for thermoplastic materials with enhanced properties [30–38].

Foam technology has been developing since 1930, using blowing agents in polymer processing. Polymer foams consist of two phases: a polymeric matrix and entrapped, well-dispersed cells generated by blowing agents. Foams have several advantages: low density, insulating capability, energy absorption, etc. These make foams a desired product in many applications such as packaging, floating materials, paddings, shields for reducing noise, shoes, etc. Foam density varies across a wide range from several kg/m^3 to near thousands kg/m^3 [39]. Carbon dioxide was used as a physical blowing agent (PBA): it has a regular solubility and is considered as an eco-friendly gas. A PBA is capable to produce a cellular structure via foaming process, and it is typically applied when blown material is in liquid stage. Cellular structure in a matrix reduces density, increasing thermal and acoustic insulation [40, 41].

The proposal of the present work is the development of biodegradable foams from PBAT/PLA blends, reinforced with bio-calcium carbonate from avian eggshells, 125 μm particle size, compatibilized with PLA gamma-radiated at 150 kGy, and further assessed for DSC, TGA, XRD, SEM, FTIR, and mechanical essays.

2. Experimental section

2.1 Materials

PLA and PBAT polymers, with main characteristics described in **Table 1**.

Both PLA and PBAT were dried at 70°C for 12 h before processing.

PLA, irradiated in a Cobalt-60 source, 150 kGy, 10.5 kGY h^{-1} dose ratio, at multipurpose reactor, in CTR/IPEN, Instituto de Pesquisas Energéticas e Nucleares, São Paulo.

Carbon dioxide (CO_2): physical blowing agent, selected according to good diffusion in PLA foaming [42].

Calcium carbonate ($CaCO_3$) from avian eggshells: white chicken eggshells were subjected to a thorough cleaning using tap water for removing of internal membranes. Afterward, clean eggshells were kept for 4 h in a 100°C water bath

Characteristics of PLA	Characteristics of PBAT
Grade: ingeo biopolymer 3251 D	Commercial name: Ecoflex FS
Supplier: nature works	Supplier: BASF
Melting point: 168°C	Melting point: 110–120°C
Glass transition temperature: 62°C	Glass transition temperature: −30°C
Average molecular weight: 100,000 g mol^{-1}	Average molecular weight: 40,000 g mol^{-1}

Table 1.
Main characteristics of used polymers.

Designation	PBAT (wt%)	PLA (wt%)	CaCO$_3$ (phr)	PLA 150 kGy (phr)
PBAT	100	—	—	—
PBAT50	50	50	—	—
PBAT65	65	35	—	—
PBAT82	82	18	—	—
PBAT50CI	50	50	10	5
PBAT65CI	65	35	10	5
PBAT82CI	82	18	10	5
PLA	—	100	—	—

Table 2.
Material designation and composition for PBAT/PLA/CaCO$_3$/PLA 150 kGy gamma-irradiated.

and finally dried at 100 ± 2°C for 2 h in an air-circulating oven. Eggshells were size reduced to fine powder, particle size equal or lower than 125 μm, by using ball mills and granulometric sieve, respectively. Then they were dried again at 100 ± 2°C, for 24 h, in order to reduce its moisture content to less than 2%.

2.2 Preparation and processing

Composite materials were prepared according to **Table 2**; they were first homogenized by melting extrusion process, using a corotating twin-screw extruder (HAAKE Rheomex 332p, 3.1 L/D, 19/33 compression ratio), by using a 120–145°C temperature profile and 50 rpm.

Homogenized samples (pellets) were further subjected to extrusion under pressure, by expansion physical method using carbon dioxide (CO_2) as blowing agent, at 10 bar (approximately 10 kgf cm^{-2}). A mono-screw specific for foaming was used, maintaining the same temperature profile: 130–145°C.

3. Characterization

3.1 Differential scanning calorimetric analyses (DSC)

Thermal behavior was examined in a DSC Mettler Toledo apparatus, according to ASTM D3418-08. A set of heating/cooling ramps was carried out following a three-step process; the samples were firstly heated to 200°C and kept in the molten state for 10 min to erase the thermal history of the material. They were then cooled

down to 30°C at 10°C min^{-1} to evaluate the ability of PLA, PBAT, and their compositions listed in **Table 2** to crystallize upon cooling. After cooling treatment, the samples were heated back to 200°C at 10°C min^{-1}. The percent crystallinity of each one was calculated separately, upon the second heating by using Eq. 1 [43]:

$$x_c \ (\%\text{Crystallinity}) \ = \ \frac{\Delta H_m}{\Delta H_m^o} \times \frac{100}{w}.$$ (1)

where ΔH_m is the measured heat of fusion, w is the weight fraction of PLA or PBAT in the blend, and $\Delta H^o{}_m$ is the enthalpy of fusion for a crystal having infinite crystal thickness (93 J g^{-1} for PLA and 114 J g^{-1} for PBAT).

3.2 Thermogravimetric analyses (TG)

Thermogravimetric analyses provide complimentary and supplementary characterization information to DSC, by measuring the amount and rate (velocity) of change in the mass of a sample as a function of temperature or time in a controlled atmosphere. Measurements are used primarily to determine the thermal and/ or oxidative stabilities of materials as well as their compositional properties. The technique can analyze materials that exhibit either mass loss or gain due to decomposition, oxidation, or loss of volatiles (such as moisture). TGA were performed using a DSC Mettler Toledo apparatus, according to ASTM E1641-07, by using 5–9 mg of foam sample, within a 25–600°C program, at 10°C min^{-1}, in a nitrogen flow of 50 ml min^{-1}.

3.3 X-ray diffraction analysis (XRD)

X-ray diffraction is a technique used for determining anatomic structure: it consists in a constructive interference of a wave from X-ray incident beam in relation to a uniform atomic spacing.

In this technique Bragg's law is applied, defined by $n\lambda = 2dsen\theta$, where $n\lambda$ is an entire value for wavelength generated by a specific target according to a given electronic transition and $sen\theta$ is the angle where the constructive interference occurs; therefore, it is possible to determine interplanar distances (d) for each crystalline plane. The identification of crystalline phase of a material is given from a database defined by the Joint Committee on Powder Diffraction Standards (JCPDS) that compares position of obtained peaks with intensity relationship.

It was employed herein a X-Ray diffractometer, RigakuMultiflex, graphite monochromator, 40 kV, 20 mA, X-rays tube, copper anode $\lambda \, Cu_{k\alpha} = 1,5418 \, \mathring{A}$, scanning 2θ within 3°–60°, speed 0.06°/4 s, fixed time. It provides, among others, information on sample crystallinity, via diffractograms, distinguishing between amorphous and crystalline states.

3.4 Scanning electron microscopy (SEM)

Electronic microscopy technique is a major tool for the study of material structure and morphology; it allows the visualization of details in a micrometric scale of changes in the material.

Morphology investigations were accomplished in a FEG-SEM equipment, model F-50, capable to read up to 20 nanometers, in various magnification micrographs. Samples were freeze-fractured in liquid nitrogen and gold coated in a Balzers SCD 050 sputtering before accomplishment of analyses.

3.5 Attenuated total reflection Fourier-transform infrared spectroscopy (ATR-FTIR)

FTIR is a sensible method for identifying chemical modification in a material and, so, is capable to detect chemical modifications in a polymeric material. This method detects vibrational movements imparted from chemical bonds for the material that is being analyzed. As each chemical group absorbs vibrational energy at a given value, it is possible to differentiate them via infrared spectrum. Spectra were obtained from a PerkinElmer, universal ATR sampling accessory spectrum 100 FTIR spectrometer. Setup collection sample was adjusted for 64 scans, within a 4000–650 cm^{-1} range.

3.6 Tensile and elongation at break

Tensile and elongation at break essay are relevant instruments for evaluating loss of properties and evolution of degradative process of the polymer. Parameters that contribute for mechanical behavior of polymers are chemical structure, crystallinity degree, molar mass, moisture, and reinforcing agent present, among others. All these properties are modified during degradation processes. In case of reinforcing agents, the concentration is not changed; nevertheless, their interaction can be modified in consequence of chemical modifications suffered by the polymer. Tensile and elongation at break tests were accomplished at 25 ± 5°C, in an EMIC model DL 300 universal essay machine, 20 kN load cell, 50 mm min^{-1}, in accordance with ASTM D 638-14. Specimens were conditioned at 25 ± 5°C and 50 ± 5% relative humidity, for 24 h, prior to testing.

4. Results and discussion

4.1 Differential scanning calorimetric analyses (DSC)

DSC heating curves of PLA, PBAT, and PLA/PBAT (50/50) blends, after crystallizing from melt, are shown in **Figure 1**.

PLA was primarily amorphous when it was cooled from melt, and this result suggests that PLA was not able to crystallize within the cooling time frame.
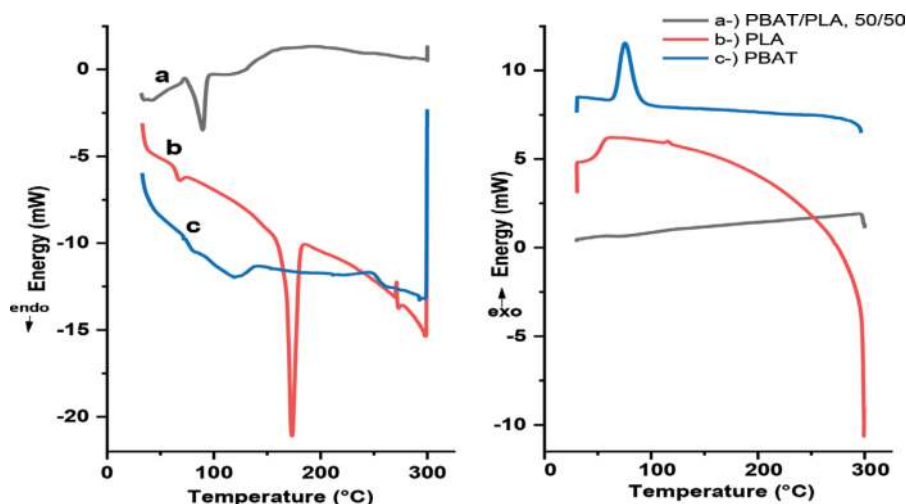

Figure 1.
Melting and crystallization curves for PLA, PBAT, and PLA/PBAT (50/50).

In **Table 3** a brief summary of thermal properties of PLA, PBAT, and PBAT/PLA (50/50) is depicted:

4.2 Thermogravimetric analyses (TG)

TG was carried out to investigate the effect of processing on the thermal decomposition of PLA and PBAT under nitrogen atmosphere; in **Figure 2** behavior of samples studied is shown.

The onset temperature of the decomposition of PLA slightly decreases with the extrusion process; nevertheless, its blend with PBAT and PBAT purely showed a higher onset temperature. This change in PLA could be originated from the degradation of the polymer, leading to the presence of shorter polymer chains and an increase in the number of chain ends per mass. Chain ends then promote a dominant degradation pathway at the temperature range of 270–360°C.

4.3 X-ray diffraction analysis (XRD)

X-ray diffraction patterns of all studied samples are shown in **Figure 3**.

In order to provide a more effective visualization of involved samples, as well as their behavior in the present study, components were separated into individual graphs, according to **Figures 4-7**, as follows.

Designation	Tg (°C)	Tm (°C)	Xc (%)
PBAT	−29.7 [44]	120.0	14.8
PLA	60.4	158.0	61.1
PBAT/PLA, 50/50	—	86.9	29.9

Tg = glass transition temperature; Tm = melting temperature, second fusion; Xc = crystallinity.

Table 3.
Thermal properties of materials studied.
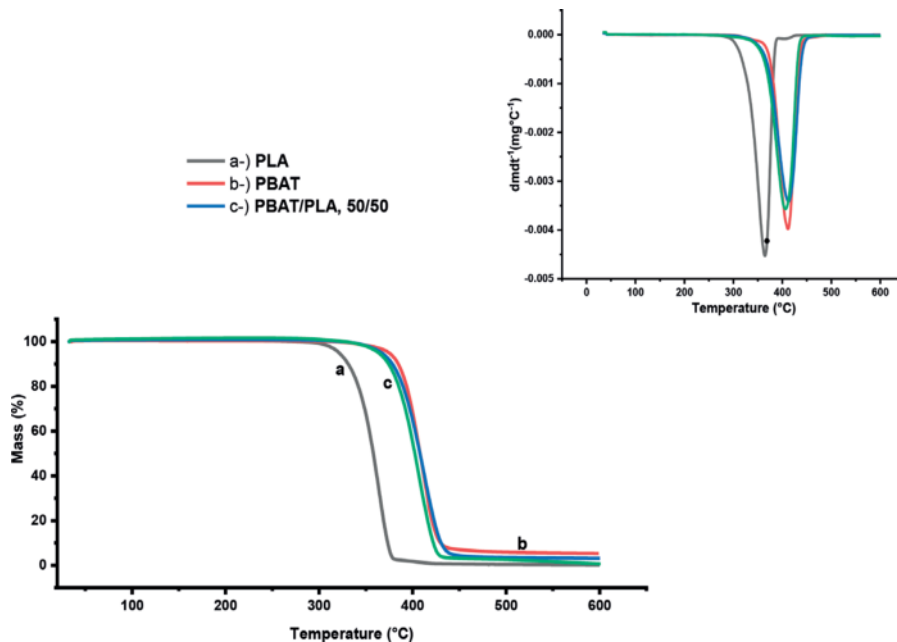
Figure 2.
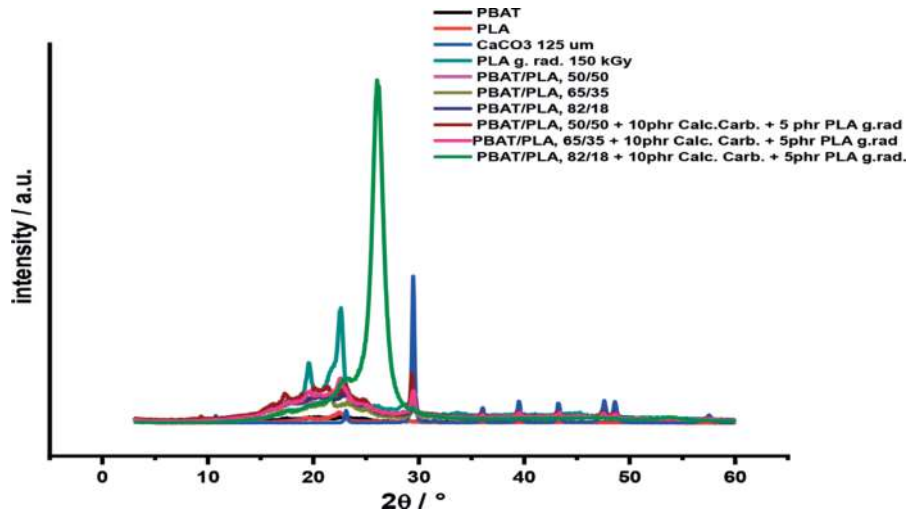*TG and DTG curves for PLA, PBAT, and PBAT/PLA (50/50).*

Figure 3.
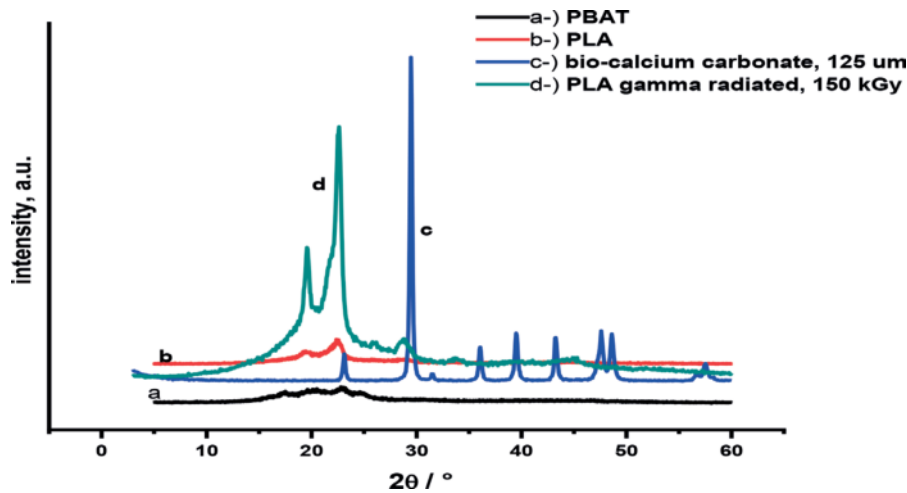*DRX diffractograms of all studied samples.*

Figure 4.
DRX diffractograms of basic components: PBAT, PLA, CaCO₃, and PLA gamma-radiated at 150 kGy.

In general, the sample is composed by crystals and amorphous phases: the sharp peaks are related to crystallite diffraction, and larger peaks are related to amorphous phases. In **Figure 4**, pure PBAT and PLA exhibited four peaks in 17.5, 20.5, 22.5, and 24.5°, in which 22.5° 2θ was the most intense. Bio-CaCO₃ exhibited the most intense peak at 30.0 2θ, among other crystalline ones. PLA gamma-irradiated at 150 kGy exhibited two peaks at 20.0 and 22.0, 2θ, proving the efficacy of gamma irradiation treatment.

PBAT/PLA blends, 82/18 and 65/35, corresponding to **Figures 5** and **6**, respectively, as well as their composites, exhibited two intense peaks at 22.5 and 30.0 2θ, emphasizing that composites showed a higher intensity for peaks than based blends.

PBAT/PLA blend (50/50) and its composite showed just one intense peak at 30.0 2θ, much more intense for corresponding composite.

4.4 Scanning electron microscopy (SEM)

The cell morphology of all formulations processed using SEM is shown in **Figures 8** and **9**. Images were taken in a 100 × magnification, confirming structural foam nature [45].
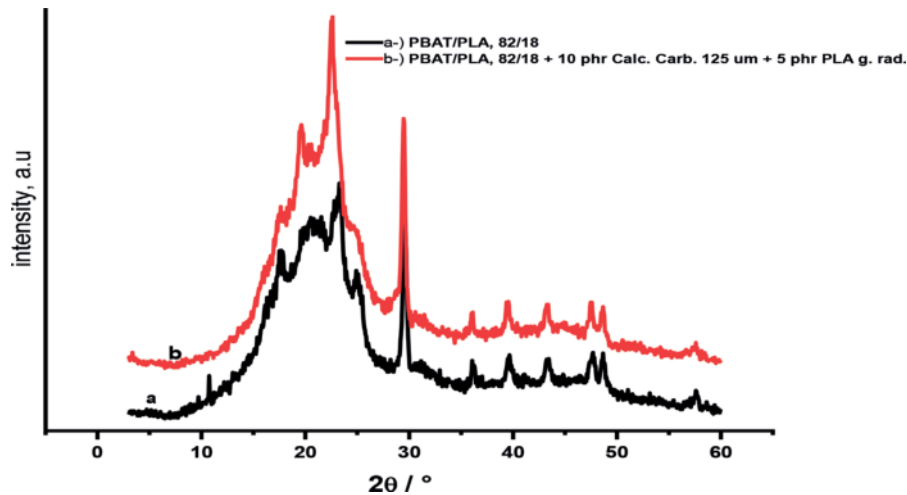
Figure 5.
DRX diffractograms of PBAT/PLA (82/18) and their compositions with 10 phr of CaCO$_3$ and 5 phr of PLA gamma-radiated at 150 kGy.
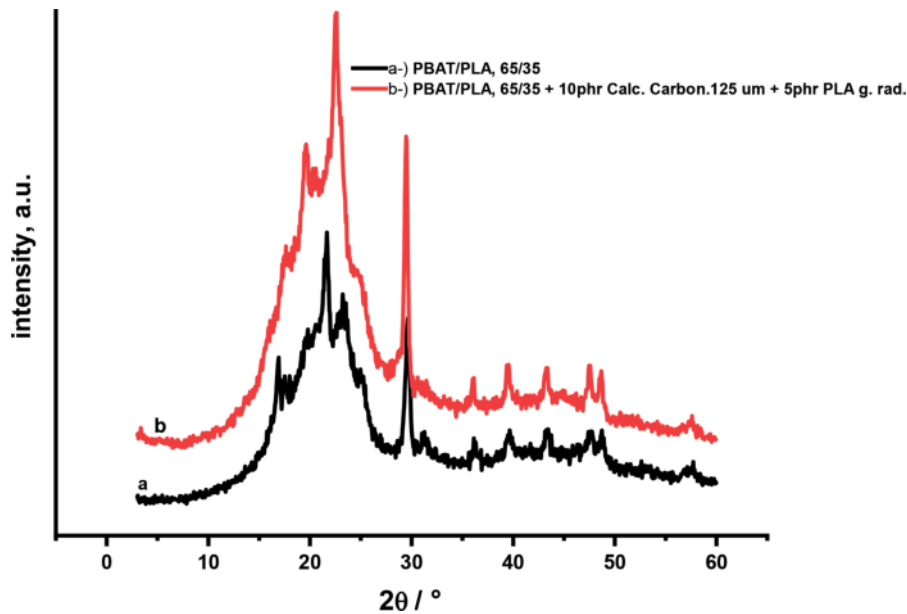

Figure 6.
DRX diffractograms of PBAT/PLA (65/35) and their compositions with 10 phr of CaCO$_3$ and 5 phr of PLA gamma-radiated at 150 kGy.

The higher PBAT concentration in PLA/PBAT blends, the easier will be the miscibility between both PBAT and PLA, as shown in **Figure 8**; in **Figure 9** pure PLA and PBAT micrographs are presented.

PLA shows an irregular dispersion and PBAT a continuous phase in blends; that is, PLA has a typical and irregular morphology *island-phase* type and the PBAT a *sea-phase* type morphology, as can be observed in **Figure 9a** and **b**.

Addition of PLA gamma-irradiated at 150 kGy contributed for an effective distribution of bio-calcium carbonate 125 μm reinforcement in PBAT/PLA compositions and buildup of structural foams, as can be seen in **Figure 10**.

In **Figure 11** foamed samples obtained from 4 mm die extruder and final specimens are shown.
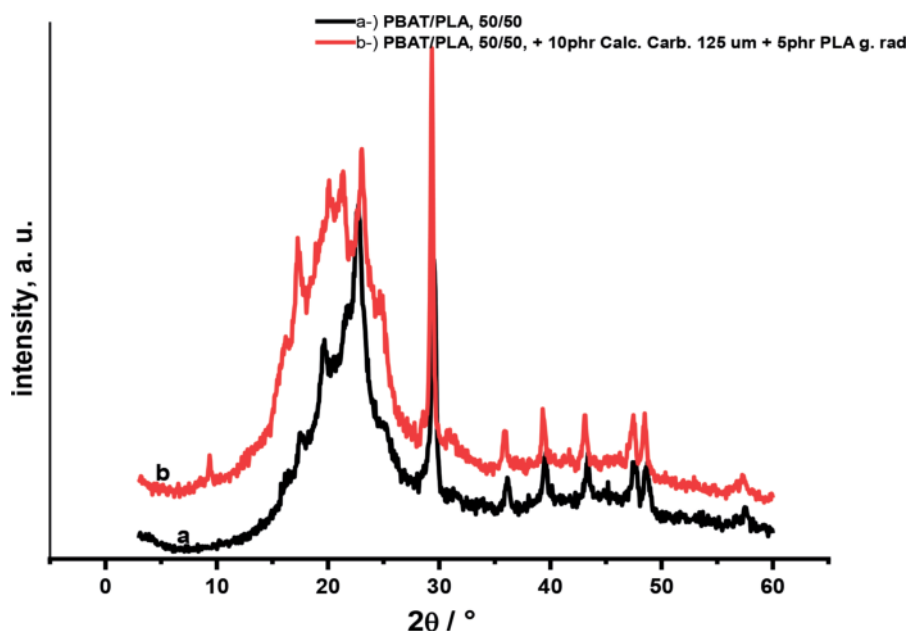
Figure 7.
DRX diffractograms of PBAT/PLA (50/50) and their compositions with 10 phr of CaCO₃ and 5 phr of PLA gamma-radiated at 150 kGy.
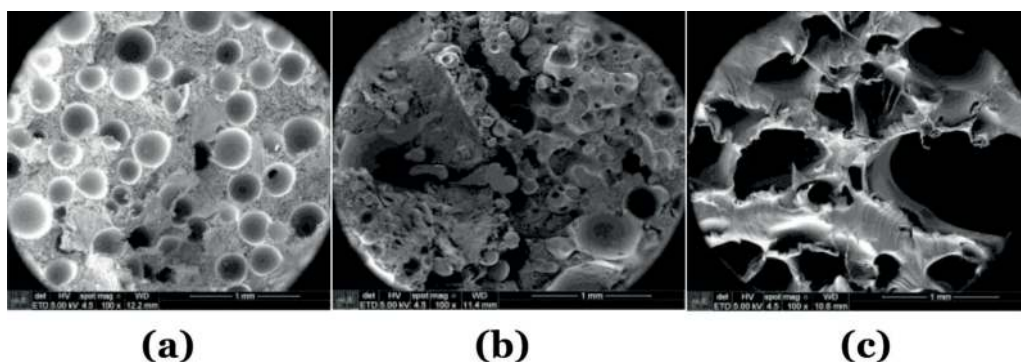

Figure 8.
SEM micrographs of PLA/PBAT blends, 100 X magnification: (a) PBAT/PLA, 82/18; (b) PBAT/PLA, 65/35; (c) PBAT/PLA, 50/50.

4.5 Attenuated total reflection Fourier-transform infrared spectroscopy (ATR-FTIR)

FTIR spectra of PBAT/PLA blends and PBAT/PLA blends with 10phr of bio-$CaCO_3$ and 5 phr of PLA gamma-radiated at 150 kGy are shown, respectively, in **Figures 12** and **13**.

For PLA, the peak at around 752 cm^{-1} associated with the rocking vibration of α-methyl; peak at around 864 cm^{-1} associated with the ester (O-CH-CH₃); the peak at around 1042, , and 1180 cm^{-1} associated with the stretching vibration of C-O-C; the peak at 1381 cm^{-1} associated with the CH symmetric bending vibration; the peak at around 1450 cm^{-1} associated with the CH₃ antisymmetric; the peak at 1748 cm^{-1} associated with the carbonyl C=O stretching vibration; and the symmetric and antisymmetric stretching vibration of CH3 of saturated hydrocarbons were found at 2943 and 2997 cm^{-1}, respectively [46, 47].

For PBAT, the peak at 725 cm^{-1} associated with the bending vibration of CH-plane of benzene ring; the symmetric stretching vibration of trans-C-O was found at 937 cm^{-1}; the peak at 1018 cm^{-1} associated with the bending vibration at the surface of adjacent hydrogen atoms on the phenyl ring; the peak at 1103 cm^{-1} associated with the left-right symmetric stretching vibration of C-O; the peak at 1265 cm^{-1} associated with the C-O symmetric stretching vibration; the peak at 1408 cm^{-1} associated with the trans-CH$_2$-plane bending vibration; the peak at 1504 cm^{-1} associated with the skeleton vibration of the benzene ring; the peak at 1713 cm^{-1} associated with the C-O stretching vibration; and the peak at 2959 cm^{-1} associated with the CH$_2$ asymmetric stretching vibration [46, 47].
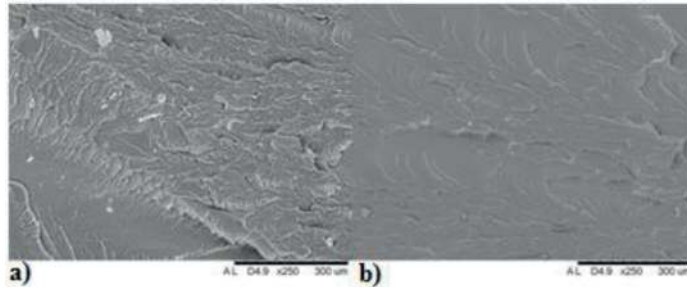

Figure 9.
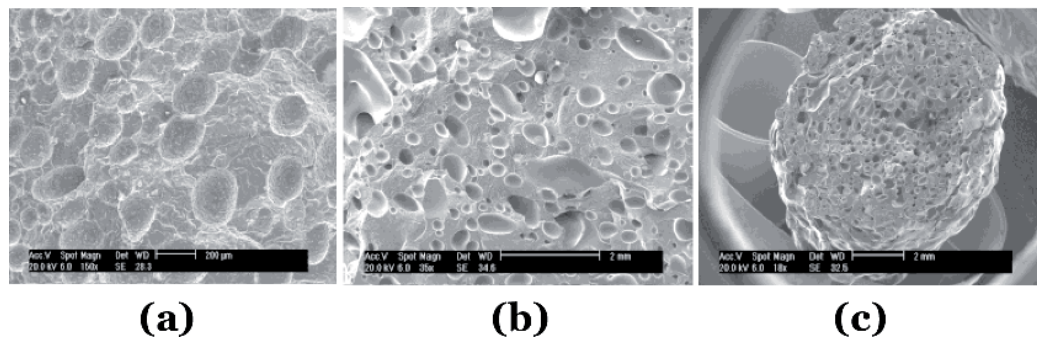*SEM micrographs, 500 X magnification, for pure PLA (a) and pure PBAT (b).*

Figure 10.
SEM micrographs of foams, randomly chosen, with different magnifications: 150 (a), 35 (b), and 18 (c) X, respectively.
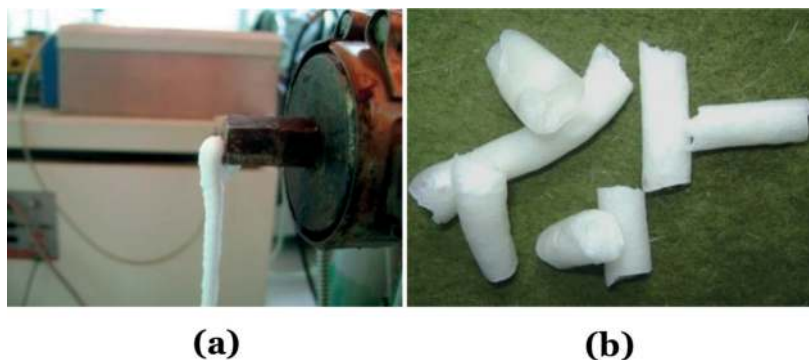

Figure 11.
Structural foams: (a) extruded foams from a 4 mm die extruder; (b) cylinder structural foams, of approximately 400 kg m^{-3} density.
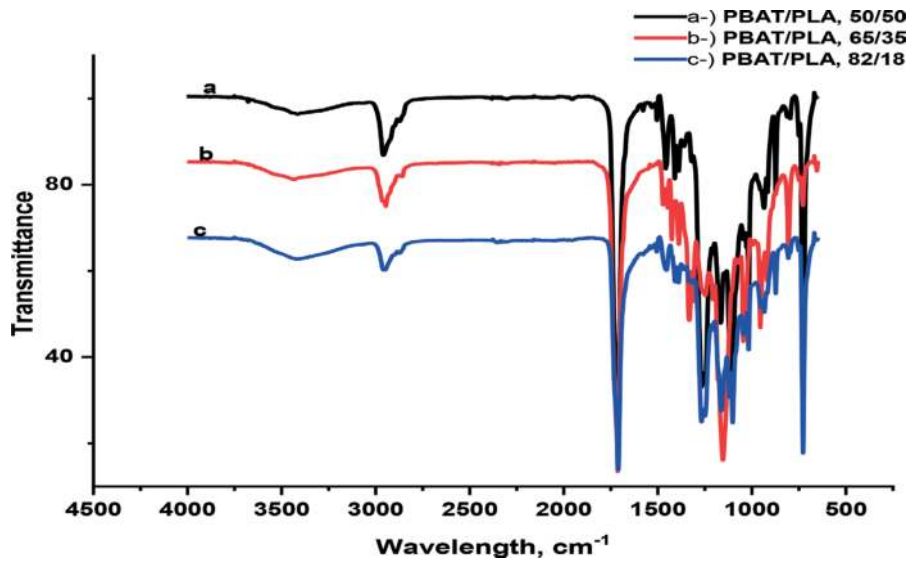
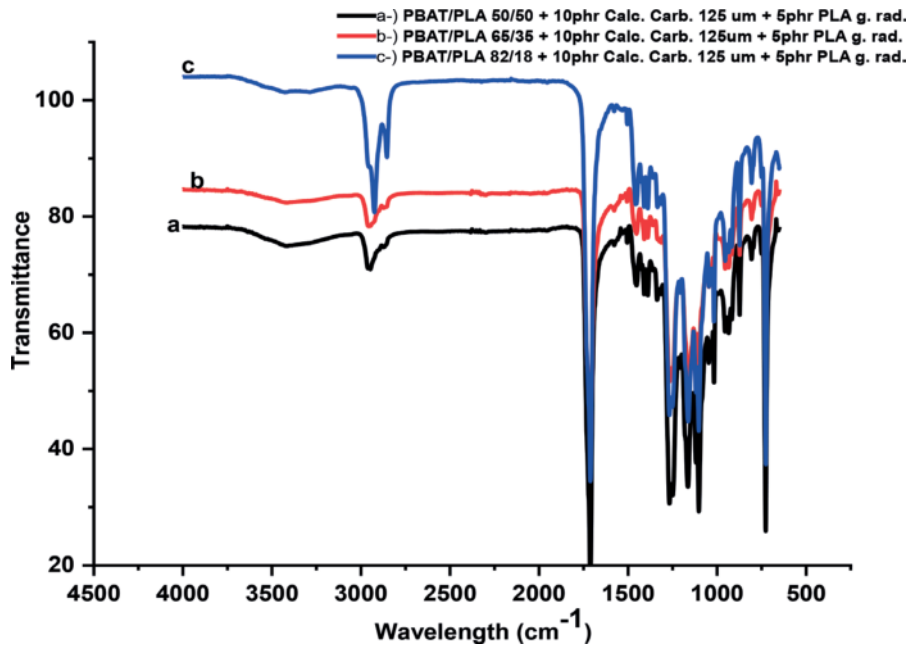**Figure 12.**
FTIR spectra of PBAT/PLA blends.

Figure 13.
FTIR of PBAT/PLA blends incorporated with c (10 phr of bio-CaCO₃) and I (5 phr of PLA gamma-radiated at 150 kGy).

Absorption spectral of PLA/PBAT blends showed the upshift of CH-plane of the benzene ring vibration from 725 to 729 cm^{-1}. Ester vibration peak in PLA shifted from 864 to 872 cm^{-1} [7]. There was however no clear evidence of interaction between PLA and PBAT in the blends.

4.6 Tensile and elongation at break

Tensile mechanical properties of PBAT/PLA blends and PBAT/PLA blends with 10 phr of bio-calcium carbonate and 5 phr of PLA gamma-radiated at 150 kGy are presented in **Figures 14** and **15**.
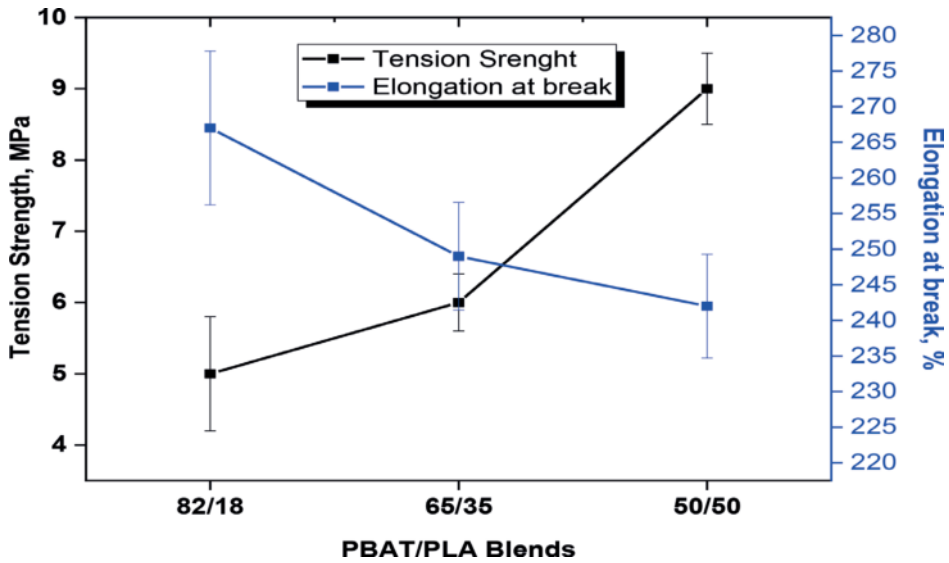
Figure 14.
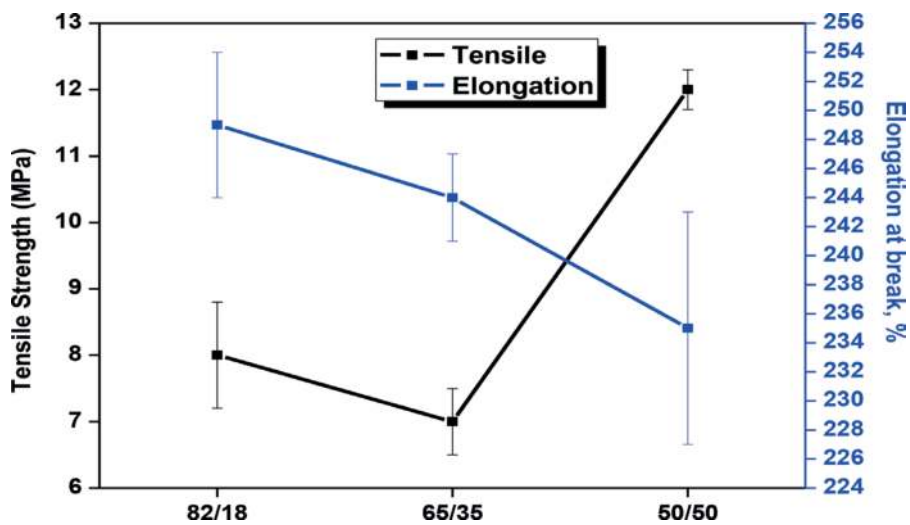*Tensile mechanical properties for PBAT/PLA blends: 82/18, 65/35, and 50/50.*

Figure 15.
PBAT/PLA blends, 82/18, 65/35, and 50/50 with 10 phr of bio-CaCO₃ and 5 phr of PLA gamma-radiated at 150 kGy.

Blends and composites	Tensile strength (MPa)	Elongation at break (%)	Elasticity modulus (MPa)
PBAT50	9.0	242.0	112.6
PBAT65	6.0	250.0	93.1
PBAT82	5.0	265.0	215.0
PBAT50CI	12.0	235.01	116.2
PBAT65CI	7.0	244.0	126.9
PBAT82CI	8.0	249.0	138.5

Table 4.
Tensile properties of PBAT/PLA blends and their composites.

13

In **Table 4** tensile properties presented in **Figures 14** and **15** are summarized.

From **Table 4**, PBAT/PLA 50/50 presented a higher value for tensile strength and PBAT/PLA 82/18 a higher value for elongation at break and elasticity modulus. PBAT/PLA compositions with bio-calcium carbonate and PLA gamma-radiated at 150 kGy presented results slightly higher than base compositions, following the same tendency.

5. Conclusions

Interaction between PLA and PBAT, registered from thermal analyses, proved to be fundamental for accomplishment of investigations. Addition of calcium carbonate from avian eggshells proved to be effective for reinforcement of PBAT/PLA blends, according to mechanical tests. PLA gamma-radiated at 150 kGy, used as compatibilizing agent, provided a higher crystallinity in assessed samples, as it can be seen from DRX analyses, exhaustively shown in separate graphs: in summary, it contributed for the effective interaction between components and further good performance in mechanical essays. Spectra obtained from infrared determinations were typical for PLA, PBAT, and their blends; nevertheless, insertion of bio-$CaCO_3$ and PLA gamma-radiated at 150 kGy contributed for more defined peaks, within 2750 and 3200 cm^{-1}. SEM analyses pointed toward the acquisition of structural closed-cell foams, with no interference of naturally immiscible PLA and PBAT; this efficacy can be attributed to PLA gamma-radiated at 150 kGy, capable to provide a complete and expected interaction between bio-$CaCO_3$ and PBAT/PLA blends.

Acknowledgements

Author details

Elizabeth C.L. Cardoso*, Duclerc F. Parra, Sandra R. Scagliusi, Ricardo M. Sales, Fernando Caviquioli and Ademar B. Lugão
Instituto de Pesquisas Energéticas e Nucleares, São Paulo, SP, Brazil

*Address all correspondence to: eclcardo@ipen.br

IntechOpen

References

[1] Jia W, Gong RH, Hogg PJ. Poly(lactic acid) fibre reinforced biodegradable composites. Composites. Part B, Engineering. 2014;**62**:104-112

[2] JalaliDil E, Carreau PJ, Favis BD. Poly(butylene adipate-co-terephthalate) blends. Polymer. 2015;**68**:202-212

[3] Pivsa-Art W, Chaiyasat A, Pivsa-Art S, Yamane H, Ohara H. Preparation of polymer blends between Poly(lactic acid) and Poly(butylene adipate-co-terephthalate) and biodegradable polymers as compatibilizers. Energy Procedia. 2013;**34**:549-554

[4] Yu T, Li Y. Influence of poly(butylene adipate-co-terephthalate) on the properties of the biodegradable composites based on ramie/poly(lactic acid), Composites. Part A, Applied Science and Manufacturing. 2014;**58**:24-29

[5] Zhao P, Liu W, Wu Q, Ren J. Preparation, mechanical and thermal properties of biodegradable polyesters/poly(lactic acid) blends. Journal of Nanomaterials. 2010;**2010**:287082

[6] Chaishome J, Brown KA, Brooks R, Clifford MJ. Thermal degradation of flax fibres as potential reinforcement in thermoplastic composites. Advanced Materials Research. 2014;**894**:32-36

[7] Chaishome J, Rattanapaskorn S. International conference on mining: Material and metallurgical engineering. 2nd. Materials Science and Engineering. 2017. p. 191

[8] Gupta A, Kumar V. New emerging trends in synthetic biodegradable polymers-polylactide: A critique. European Polymer Journal. 2007;**43**(10):4053e74

[9] Klemm D, Heublein B, Fink HP, Bohn A. Cellulose: fascinating biopolymer and sustainable raw material edition. Angewandte Chemie, International Edition. 2005;**44**:3358

[10] Habibi Y, Lucia LA, Rojas OJ. Cellulose nanocrystals: Chemistry, self-assembly and applications. Chemical Reviews. 2010;**110**:3479

[11] Dufresne A. Nanocellulose: A new ageless bionanomaterial. Materials Today. 2013;**16**:220

[12] Azizi Samir MAS, Alloin F, Dufresne A. Review of recent research into cellulosic whiskers, their properties and their application in nanocomposite field. Biomacromolecules. 2005;**6**:612

[13] Nonato RV, Mantelatto PE, Rossell CEV. Production of biodegradable plastic (PHB), sugar and ethanol in a sugar mill. Applied Microbiology and Biotechnology. 2001;**57**:1

[14] Ravi Kumar MN. A review of chitin and chitosan applications. Reactive and Functional Polymers. 2000;**46**:1

[15] Blackburn RS. Natural polysaccharides and their interactions with dye molecules: Applications in effluent treatment. Environmental Science & Technology. 2004;**38**:4905

[16] Rodrigues BVM, Silva AS, Melo GFS, Vasconscellos LMR, Marciano FR, Lobo AO. Influence of low contents of superhydrophilic MWCNT on the properties and cell viability of electrospun poly(butylene adipate-co-terephthalate) fibers. Materials Science and Engineering. 2016;**59**:782

[17] Van de Velde K, Kiekens P. Biopolymers: Overview of several properties and consequences on their applications. Polymer Testing. 2002;**21**:433

[18] Gross RA, Kalra B. Influencing factors and process on in situ

degradation of Poly (Butylene succinate) film by strain biomectria ochroleuca, BFM-X1 in soil. Science. 2002;**297**:803

[19] Pereira da Silva JS, Farias da Silva JM, Soares BG, Livi S. Fully biodegradable composites based on poly (butylene adipate-coterephthalate)/ peach palm trees fiber. Composites: Part B. 2017;**129**:117

[20] Santana-Melo GF, Rodrigues BVM, da Silva E, Ricci R, Marciano FR, Webster TJ, et al. Electrospun ultraphin PBAT/nHap fibers influenced the in vitro and improved the mechanical properties of neoformed bone. Colloids and Surfaces, B: Biointerfaces. 2017;**155**:544

[21] de Castro JG, Rodrigues BVM, Ricci R, Costa MM, Ribeiro AFC, Marciano FR, et al. Designing a novel nanocomposite for bone tissue engineering using electrospun conductive PBAT/polypyrrole as a scaffold to direct nanohydroxyapatite electrodeposition. RSC Advances. 2016;**6**:32615

[22] Fukushima K, Wu MH, Bocchini S, Rasyda A, Yang MC. PBAT based nanocomposites for medical and industrial applications. Materials Science and Engineering: C. 2012;**32**:1331-1351

[23] Chen JH, Chen CC, Yang MC. Characterization of nanocomposites of poly (butylene adipate-co-terephthalate) blending with organoclay. Journal of Polymer Research. 2011;**18**:2151-2159

[24] Alexandre M, Dubois P. Polymer-layered silicate nanocomposites: Preparation, properties and uses of a new class of materials. Materials Science and Engineering. 2000;**28**(1e2):1e63

[25] Maazouz A, Lamnawar K, Mallet B. Improvement of thermal, stability, rheological and mechanical properties of PLA, PBAT and their blends by reactive extrusion with functionalized epoxy, polymer, degradation and stability. International Journal of Engineering Science. 2012;**XXX92012**:1-17

[26] Lamnawar K, Maazouz A, Mallet B. Patent; 2010. International patent C08J5/

[27] Gu SY, Zhang K, Ren J, Zhan H. Melt rheology of polylactide/ poly(butylene adipate-co-terephthalate) blends. Carbohydrate Polymers. 2008;**74**(1):79e85

[28] Global poultry trends: "Asia is a key to global egg output growth". The Global Poultry Site. 2013. Available from: http://www.thepoultrysite.com/ articles/2735/global-poultry-trends-asia-is-key-to-global-egg-output-growth

[29] Hassan SB, Aigbodion VS, Patrick SN. Development of polyester egg shell particulate composites. Tribology in Industry. 2012;**34**(4):217-225

[30] Guven O et al. Polymer recycling: Potential application of radiation technology. Radiation Physics and Chemistry. 2002;**64**(1):41-51

[31] Sun Y, Chmielewski AG. Applications of Ionizing Radiation in Materials Processing. Institute of Nuclear Chemistry and Technology. Warszawa, Erasmus; Vol. 2. 2017

[32] Rangari VK et al. Value added biopolymer nanocomposites from waste eggshell-based $CaCO_3$ nano particles as fillers. ACS Sustainable Chemistry & Engineering. 2014;**2**(4):706-717

[33] Utracki LA. Polymer blends, rapra review report, 11, Report 123. 2000

[34] Sonnier R, Rouif S, Taguet A. Modification of polymer blends by E-beam and gamma irradiation. 2012.

Available from: www.researcggate.net/
publication/285296722

[35] Makuuchi K, Cheng S. Radiation
Processing of Polymer Materials and its
Industrial Applications. Nova York: John
Wiley & Sons Inc; 2012. p. 1

[36] Chmielewski A, Haji-Saeid M.
Radiation technologies: Past, present
and future. Radiation Physics and
Chemistry. 2004;**71**:17

[37] Zhao W, Pan X. Technology
of Radiation Processing and its
Applications. Beijing, China: Weapon
Industry; 2003

[38] Telnov AV, Zavyalov NV,
Khokhlov YA, Sitnikov NP, Smetanin
ML, Tarantasov VP, et al. Radiation
degradation of spent butyl rubbers.
Radiation Physics and Chemistry.
2002;**63**:245

[39] Zhang Y. Polyolefin formulations for
improved foaming: effect of molecular
structure and material properties
[unpublished doctoral dissertation].
Ontario, Canada: Queen's University
Kingston; 2013

[40] de Vries DVWM. Characterization of
polymeric foams. MT 09.22-0611747. 2009

[41] Borealis AG. Daploy^{TM} High Melt
Strength PP. 2004

[42] Gendron R, Mihai M. Extrusion
foaming of polylactide. In: Polymeric
Foams: Innovations in Processes,
Technologies and Products. 2016.
Available from: https://www.research
gate.net/publication/310646111

[43] Garlotta D. A literature review of
Poly(lactic acid). Journal of Polymers
and the Environment. 2002;**9**(2):63

[44] Sikorska W et al. Forensic
engineering of advanced polymeric
materials—Part V: Prediction studies
of aliphatic—Aromatic copolyester and

polylactide commercial blends in view
of potential applications as compostable
cosmetic packages. Polymers. 2017;**9**:257

[45] Cardoso ECL. Desenvolvimento de
espumas parcialmente biodegradáveis
a partir de blendas de PP/HMSPP
com polímeros naturais e sintéticos
[tese]. São Paulo: Instituto de Pesquisas
Energéticas e Nucleares (IPen)/
Universidade de São Paulo (USP); 2014

[46] Weng YX, Jin YJ, Meng QY, Wang
L, Zhang M, Wang YZ. Biodegradation
behavior of PBAT, PLA and their blend
under soil conditions. Polymer Testing.
2013;**32**(5):918-926

[47] Xiuyu M, Yufeng W, Jianqing
W, Yaning X. In: MATEC Web of
Conferences; 88, 02009. 2017